

$\pi\pi$ scattering at Large N_c

Jorge Baeza-Ballesteros,^{a,*} Pilar Hernández^a and Fernando Romero-López^{a,b}

^aIFIC, CSIC-Universitat de València,
46980 Paterna, Spain.

^bCenter for Theoretical Physics, Massachusetts Institute of Technology,
Cambridge, MA 02139, USA.

E-mail: jorge.baeza@uv.es, m.pilar.hernandez@uv.es, fromerol@mit.edu

We study the Large N_c scaling of pion-pion scattering amplitudes for $N_f = 4$ degenerate quark flavors. We focus on the standard isospin-2 channel and an additional representation that is antisymmetric in both quarks and antiquarks—the AA channel. The latter only exists for $N_f \geq 4$ and a representative state is $\frac{1}{\sqrt{2}}(|D_s^+\pi^+\rangle - |D^+K^+\rangle)$. We compare the results obtained for two regularizations (Wilson and twisted-mass fermions) and three values of the lattice spacing, and observe significant discretization effects in the AA channel. Finally, we match our results to NLO SU(4) and NNLO U(4) chiral perturbation theory and constrain the N_c scaling of the relevant low-energy constants.

*The 38th International Symposium on Lattice Field Theory, LATTICE2021 26th-30th July, 2021
Zoom/Gather@Massachusetts Institute of Technology
Report number: IFIC/21-42, MIT-CTP/5345*

*Speaker

1. Introduction

The 't Hooft limit of QCD [1], that is, the limit of large number of colors, N_c , is a simplification of the theory of strong interactions. It captures most of the non-perturbative features of QCD, such as asymptotic freedom, spontaneous chiral symmetry breaking, confinement, or the existence of a low-energy spectrum of pseudo-Goldstone bosons. Moreover, it has proven to have predictive power in the non-perturbative regime, and is often used in phenomenological approaches to QCD.

Several studies have addressed the Large N_c limit via lattice simulations [2]. Particularly interesting are questions where Large N_c predictions seem to fail, such as non-leptonic kaon decays. Intrinsic QCD effects in these processes at Large N_c have been recently studied by our group [3], finding that subleading N_c corrections can naturally account for the discrepancy. However, final state interactions might also be relevant and remain to be studied. Another interesting open question is whether exotic states such as tetraquarks survive in the Large N_c limit. Both these questions can be explored studying scattering processes on the lattice.

In this talk we report the current state of our study of $\pi\pi$ scattering at Large N_c . We work in a theory with $N_f = 4$ degenerate quark flavors, for which seven different irreducible representations (irreps) of $SU(4)_f$ exist [4]. We have focused on two of them:

- The 84-dimensional irrep, which is the analogous to the isospin-2 ($I = 2$) channel of $SU(2)_f$. A representative state for this channel is the well-known $|\pi^+\pi^+\rangle$.
- The 20-dimensional irrep, which only exists for $N_f \geq 4$ and is antisymmetric in quarks and antiquarks. We refer to it as the AA channel. A representative state is $\frac{1}{\sqrt{2}}(|D_s^+\pi^+\rangle - |D^+K^+\rangle)$.

For these two channels, two-pion correlation functions are computed on the lattice as linear combinations of the disconnected and connected quark contractions—see Fig. 1:

$$C_{I=2} = 2D - 2C, \quad C_{AA} = 2D + 2C. \tag{1}$$

From the lattice results, we extract scattering properties and match them to chiral perturbation theory to constrain the Large N_c scaling of the relevant low energy constants.

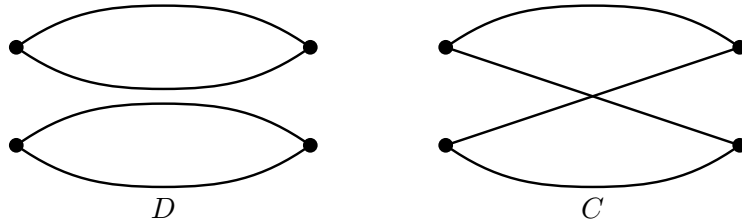


Figure 1: Schematic representation of the disconnected (left) and connected (right) quark contractions required to compute the two-pion correlators in the lattice for the $I = 2$ and AA channels.

2. $\pi\pi$ scattering in ChPT

Chiral perturbation theory (ChPT) is an effective theory that describes the low-energy behavior of QCD in terms of the lightest non-singlet multiplet of mesons and a finite number of low-energy

constants (LECs). These mesons are the pseudo-Goldstone bosons resulting from the pattern of spontaneous chiral symmetry breaking of QCD, $SU(N_f)_L \times SU(N_f)_R \rightarrow SU(N_f)_V$. ChPT has been widely studied [5, 6] and in the case of degenerate quarks, $\pi\pi$ scattering amplitudes are known up to next-to-next-to-leading-order (NNLO) [4]. From these results, the (s -wave) scattering lengths of the two channels of interest for $N_f = 4$ can be extracted at next-to-leading order (NLO):

$$M_\pi a_0^{I=2} = -\frac{M_\pi^2}{16\pi F_\pi^2} \left[1 - \frac{16M_\pi^2}{F_\pi^2} L_{I=2} + \frac{M_\pi^2}{32\pi^2 F_\pi^2} \left(\frac{13}{4} \ln \frac{M_\pi^2}{\mu^2} - \frac{3}{4} \right) \right], \quad (2)$$

$$M_\pi a_0^{AA} = \frac{M_\pi^2}{16\pi F_\pi^2} \left[1 - \frac{16M_\pi^2}{F_\pi^2} L_{AA} - \frac{M_\pi^2}{32\pi^2 F_\pi^2} \left(\frac{21}{4} \ln \frac{M_\pi^2}{\mu^2} + \frac{5}{4} \right) \right], \quad (3)$$

where M_π and F_π are the pion mass and decay constants, respectively, and $L_{I=2}$ and L_{AA} are linear combinations of LECs. We can expand them as a power series in N_c ,

$$L_{I=2} = N_c L^{(0)} + L_{I=2}^{(1)} + \mathcal{O}(N_c^{-1}), \quad L_{AA} = N_c L^{(0)} + L_{AA}^{(1)} + \mathcal{O}(N_c^{-1}). \quad (4)$$

Note that the leading dependence of both quantities is expected to be the same. Only leading and subleading N_c terms will be kept when matching lattice results to ChPT.

In the 't Hooft limit, we must include singlet meson, the η' , in the effective theory. Its mass originates from the explicit breaking of the $U(1)_A$ symmetry by the anomaly, which is suppressed at Large N_c . Thus, it becomes degenerate with the rest of mesons,

$$M_{\eta'}^2 = M_\pi^2 + \frac{2N_f \chi_{\text{top}}}{F_\pi^2} \xrightarrow{\text{Large } N_c} M_\pi^2 + \mathcal{O}(N_c^{-1}). \quad (5)$$

where χ_{top} is the topological susceptibility of pure Yang-Mills and $F_\pi^2 \sim \mathcal{O}(N_c)$.

An extension of ChPT to Large N_c has already been studied and is sometimes referred to as Large N_c or $U(N_f)$ ChPT [7]. It includes the η' in the pion matrix and N_c in the counting scheme, $\mathcal{O}(m_q) \sim \mathcal{O}(M_\pi^2) \sim \mathcal{O}(p^2) \sim \mathcal{O}(N_c^{-1})$, with m_q the quark mass and p the external momentum. As a consequence, loop diagrams first enter the computations at NNLO.

Within this theory, we have computed the scattering amplitudes for both channels of interest at NNLO. For $N_f = 4$ the corresponding scattering lengths are:

$$M_\pi a_0^{I=2} = -\frac{M_\pi^2}{16\pi F_\pi^2} \left\{ 1 - \frac{16M_\pi^2}{F_\pi^2} L_{I=2} + K_{I=2} \left(\frac{M_\pi^2}{F_\pi^2} \right)^2 + \frac{M_\pi^2}{32\pi^2 F_\pi^2} \left[\frac{15M_\pi^2 - 13M_{\eta'}^2}{4(M_\pi^2 - M_{\eta'}^2)} \ln \frac{M_\pi^2}{\mu^2} + \frac{M_\pi^2 - 3M_{\eta'}^2}{4(M_\pi^2 - M_{\eta'}^2)} \ln \frac{M_{\eta'}^2}{\mu^2} - \frac{1}{2} \right] \right\}, \quad (6)$$

$$M_\pi a_0^{AA} = \frac{M_\pi^2}{16\pi F_\pi^2} \left\{ 1 - \frac{16M_\pi^2}{F_\pi^2} L_{AA} + K_{AA} \left(\frac{M_\pi^2}{F_\pi^2} \right)^2 - \frac{M_\pi^2}{32\pi^2 F_\pi^2} \left[\frac{15M_\pi^2 - 21M_{\eta'}^2}{4(M_\pi^2 - M_{\eta'}^2)} \ln \frac{M_\pi^2}{\mu^2} + \frac{M_\pi^2 + 5M_{\eta'}^2}{4(M_\pi^2 - M_{\eta'}^2)} \ln \frac{M_{\eta'}^2}{\mu^2} + \frac{3}{2} \right] \right\}, \quad (7)$$

where $K_{I=2}$ and K_{AA} are combinations of $SU(N_f)$ LECs and new ones from the $U(N_f)$ theory. They scale as $\mathcal{O}(N_c^2)$ and only the leading dependence is considered as a fitting parameter when matching to lattice results.

One can compare the results of SU(4) and U(4) ChPT. In Fig. 2 we represent the scattering length in the $I = 2$ channel for both theories and two values of N_c . We have set $K_{I=2} = 0$ for the comparison and matched the values of the SU(4) and U(4) LECs using the $M_{\eta'} \gg M_\pi$ limit. The differences observed vary with N_c as a result of two effects. First, the contribution from chiral logarithms including the η' increases as $M_{\eta'}$ approaches M_π , but at the same time, the importance of the NNLO corrections gets reduced with N_c .

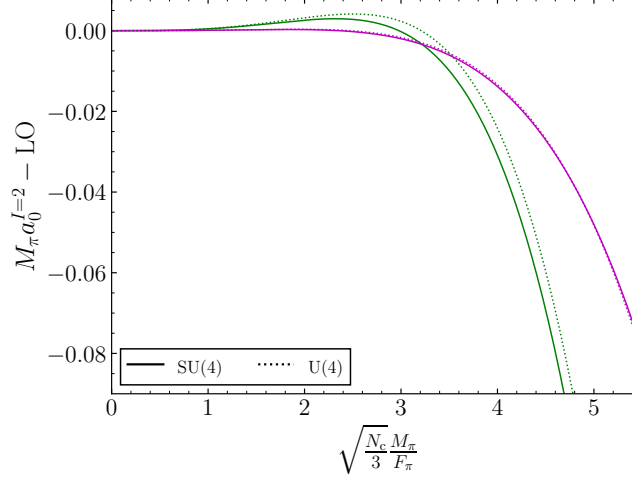


Figure 2: Comparison between the SU(4) and U(4) ChPT one-loop predictions for the scattering length in the $I = 2$ channel for $N_c = 3$ (green) and $N_c = 6$ (pink). We have set $K_{I=2} = 0$ and matched $L_{I=2}^{(1)}$ between both theories using the $M_{\eta'} \gg M_\pi$ limit.

3. Finite-volume formalism

Lattice simulations allow one to obtain the energy spectrum of two pions in a finite volume. It must then be related to infinite-volume scattering observables, such as the scattering amplitude. This is done using Lüscher’s formalism [8]. For the lowest-energy state, the s -wave phase shift, δ_0 , can be related to the ground-state energy of two pions, $E_{\pi\pi}$, on a cubic box of side L , as

$$k \cot \delta_0 = \frac{1}{\pi L} \mathcal{Z} \left(\frac{Lk}{2\pi} \right), \tag{8}$$

where k is the center-of-mass (CM) momentum, defined from $E_{\pi\pi} = \sqrt{k^2 + M_\pi^2}$, and \mathcal{Z} is the generalized Lüscher’s zeta function.

Near threshold, the energy shift of the ground state, $\Delta E_{\pi\pi} = E_{\pi\pi} - 2M_\pi$, can be expanded in terms of the s -wave scattering length, a_0 , and effective range, r_0 , of the system.

$$\Delta E_{\pi\pi} = -\frac{4\pi a_0}{M_\pi L^3} \left[1 + c_1 \left(\frac{a_0}{L} \right) + c_2 \left(\frac{a_0}{L} \right)^2 + c_3 \left(\frac{a_0}{L} \right)^3 + \frac{2\pi r_0 a_0}{L^3} + \frac{\pi a_0}{M_\pi^2 L^3} \right], \tag{9}$$

where c_1 , c_2 and c_3 are known numerical constants. This result was first developed up to $\mathcal{O}(L^{-5})$ in Ref. [8], and the order $\mathcal{O}(L^{-6})$ was later worked out in Ref. [9].

4. Energy spectrum from lattice simulations

Our lattice ensembles have been generated using HiRep [10]. We have 17 ensembles with $N_c = 3 - 6$ and lattice spacing $a = 0.075$ fm. We have also produced 4 finer ensembles for $N_c = 3$, two with $a = 0.065$ fm, and another two with $a = 0.059$ fm, which are used to study discretization effects. We used the Iwasaki gauge action with $N_f = 4$ clover-improved Wilson fermions on the sea, and two different regularizations for the valence sector:

- A unitary setup with improved Wilson fermions.
- A mixed-action setup at maximal twist.

Both are expected to show $\mathcal{O}(a^2)$ improvement and represent an extra handle to analyze possible discretization effects, since they must coincide in the continuum. Moreover, the mixed-action setup allows us to compute F_π from the one-pion correlation function. A summary of the ensembles can be found in Refs. [3, 11, 12].

In each ensemble, we compute the one- and two-pion correlators, C_π and $C_{\pi\pi}$, respectively, for both channels. We then obtain the ground state energy shift by fitting to the following ratio function [13]:

$$R(t) = \frac{C_{\pi\pi}(t+a) - C_{\pi\pi}(t-a)}{C_\pi^2(t+a) - C_\pi^2(t-a)} \xrightarrow{T/2 > t \gg 1} A_{\pi\pi} [\cosh(\Delta E_{\pi\pi} t') + \sinh(\Delta E_{\pi\pi} t') \coth(2M_\pi t')], \quad (10)$$

where $A_{\pi\pi}$ is a dimensionless amplitude, $t' = t - T/2$ and T is the time extent of the lattice. Two examples of the results of the fits are shown in Fig. 3 for different fitting ranges. The energy shifts are extracted from where a plateau is observed.

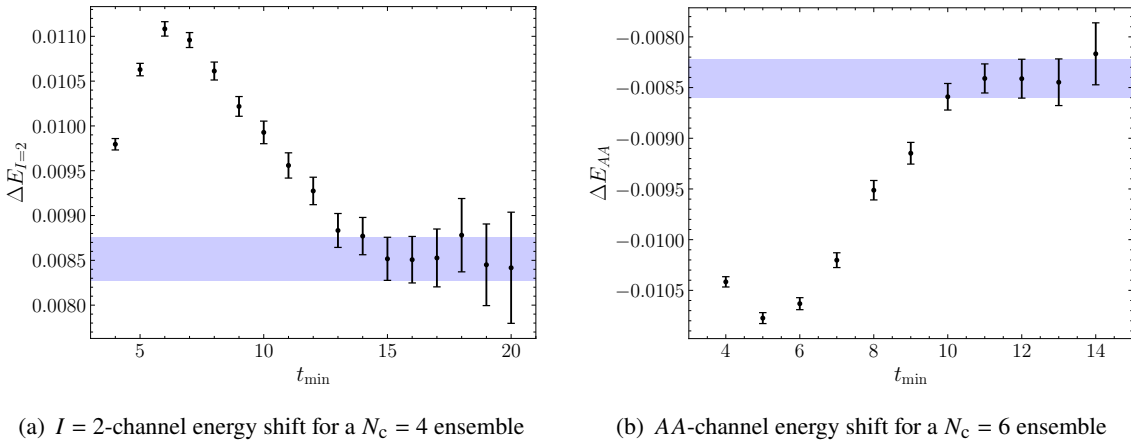


Figure 3: Energy shifts for different fitting ranges. The final result (blue) is extracted from the plateau.

For $N_c = 3$, we study possible discretization effects. In Fig. 4 we compare between both regularizations of the valence sector. We observe that discretization effects are small for the $I = 2$ channel (left), while they are as big as $\sim 50\%$ for the coarser ensembles in the AA channel (right), and get reduced for decreasing a^2 . To better understand these effects, we perform a continuum extrapolation for $N_c = 3$ in the AA channel. We use $k \cot \delta_0$ as our physical observable for this analysis and proceed in three steps:

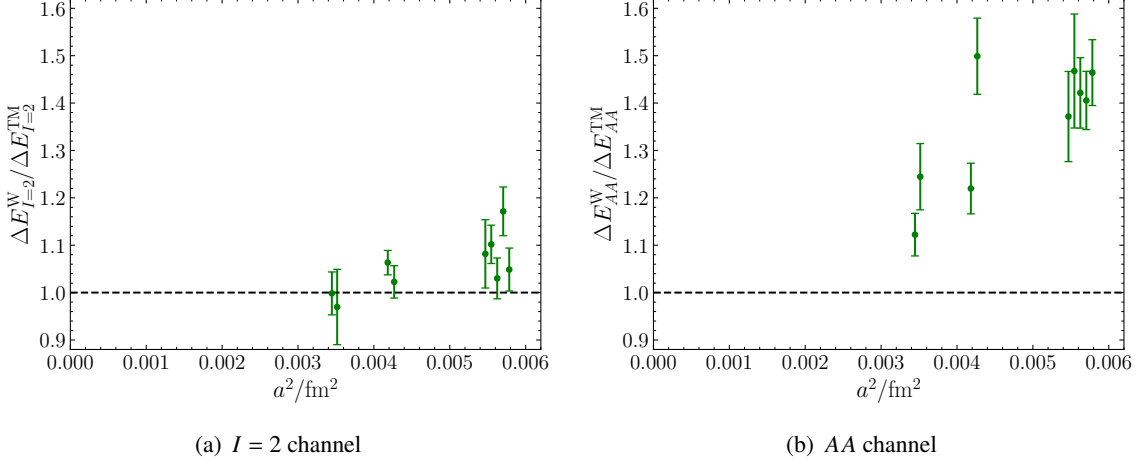


Figure 4: Dependence on the lattice spacing of the ratio between the energy shifts obtained for the unitary Wilson and the mixed-action setups.

1. First, we extrapolate all data points to a fixed value of the CM momentum, $k/M_\pi = -0.08$. We use the effective range expansion (ERE) and a prior for the effective range, $M_\pi^2 a_0 r_0 \in [-5, -1]$, motivated by the LO prediction of ChPT,

$$M_\pi^2 a_0 r_0 \Big|_{\text{LO ChPT}} = -3 \quad (I = 2 \text{ and } AA \text{ channel}). \quad (11)$$

2. For each lattice spacing, we interpolate to a fixed value of the chiral parameter, $\xi = M_\pi^2 / (4\pi F_\pi)^2 = 0.14$.
3. Finally we do a constrained linear continuum extrapolation, as shown in Fig. 5.

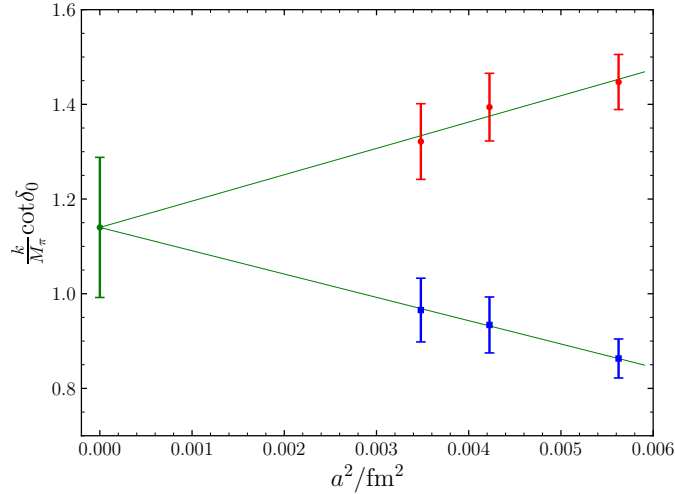


Figure 5: Continuum extrapolation of the s -wave phase shift for $N_c = 3$ in the AA channel. Results from the unitary (blue squares) and the mixed-action (red dots) setup setups are fitted simultaneously with a constrained common continuum limit.

We observe that our results are consistent with a universal continuum limit and that $\mathcal{O}(a^2)$ discretization effects are large for both regularizations. We decide to use the mixed-action results for the following analysis and parametrize the discretization effects in the scattering amplitude as

$$\mathcal{M}_{AA}^{\text{latt}} = \mathcal{M}_{AA}^{\text{cont}} + a^2 W \xi, \quad (12)$$

which is inspired in a modification of ChPT that includes the effects of Wilson fermions and a twisted mass [14, 15]. Here, W is a linear combination of new LECs appearing in this theory and obeys $W \sim \mathcal{O}(1)$ in N_c . It is treated as a fitting parameter when matching lattice results to ChPT.

5. Fits to ChPT

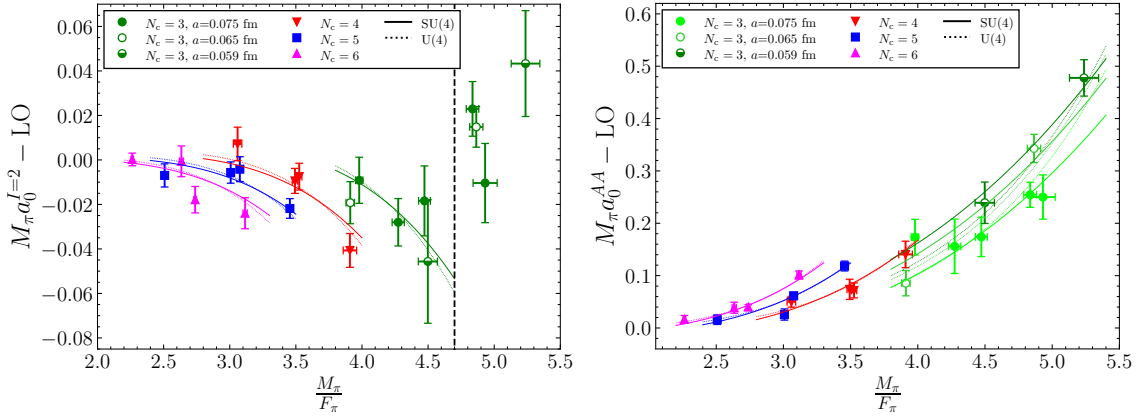
We now compare our results to ChPT to constrain the N_c scaling of the LECs. First, Eq. (9) is used to $\mathcal{O}(L^{-5})$ to extract $M_\pi a_0$ from the energy spectra and do a simultaneous chiral and N_c fit to ChPT. The results are shown in Fig. 6 for both channels and both SU(4) and U(4) theories. In the $I = 2$ channel, none of them can explain the behavior of the most massive $N_c = 3$ points, so we exclude them from the fits. Our preliminary results for the LECs in the SU(4) case are:

$$\begin{aligned} L_{I=2}/N_c \times 10^3 &= -0.11(4) - 1.43(16)/N_c, & \chi^2/\text{dof} &= 1.00, \\ L_{AA}/N_c \times 10^3 &= -1.08(13) + 2.2(3)/N_c, & \chi^2/\text{dof} &= 2.00, \end{aligned} \quad (13)$$

and in U(4) ChPT:

$$\begin{aligned} L_{I=2}/N_c \times 10^3 &= -0.10(7) - 1.29(16)/N_c, & \chi^2/\text{dof} &= 0.94, \\ L_{AA}/N_c \times 10^3 &= -0.6(4) + 2.4(3)/N_c, & \chi^2/\text{dof} &= 1.42. \end{aligned} \quad (14)$$

For both the SU(4) and U(4) ChPT fits, there is some discrepancy between the leading dependence of the LECs in both channels, which was expected to be the same.



(a) $I = 2$ channel. Points to the right of the dashed line are not considered for the fit.

(b) AA channel. Discretization effects are included as a fitting parameter.

Figure 6: Preliminary results for the simultaneous chiral and N_c fits of the scattering length to SU(4) (solid line) and U(4) (dashed line) ChPT.

We decide to study the possible impact of neglected higher-order terms in Eq. (9). The analysis is represented for two ensembles, one for each channel, in Fig. 7. We compare the threshold expansion to $\mathcal{O}(L^{-5})$ (in red) and $\mathcal{O}(L^{-6})$ (in green) using Eq. (11) for r_0 . The blue region depicts the energy shift computed in the lattice and the points are the determinations of $M_\pi a_0$. We observe that the $I = 2$ channel shows good agreement between both truncation orders. However, this is not the case for the AA channel for which convergence fails at large ξ or small volume.

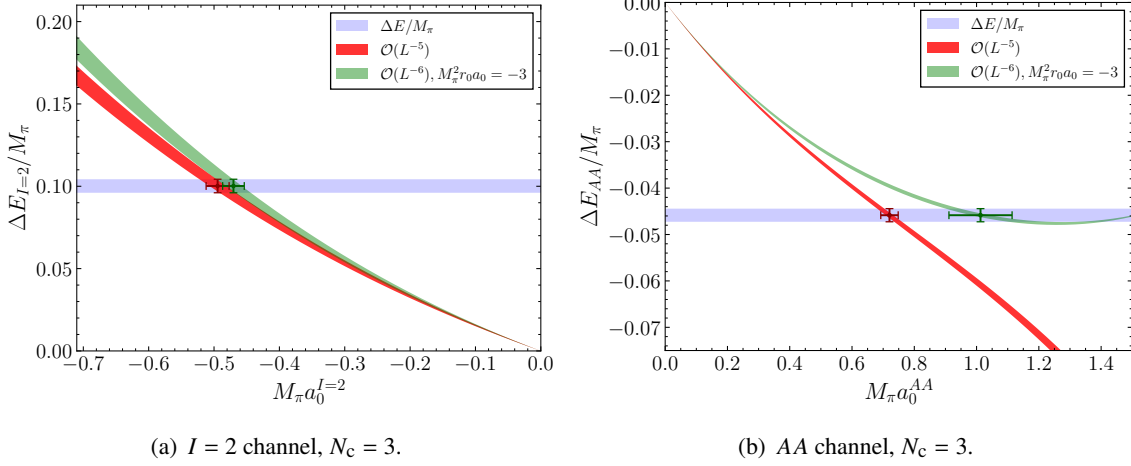


Figure 7: Comparison between the $\mathcal{O}(L^{-5})$ (red) and $\mathcal{O}(L^{-6})$ (green) threshold expansion—see Eq. (9). The horizontal blue region is the ground-state energy shift from the lattice and points are the determinations of the scattering length.

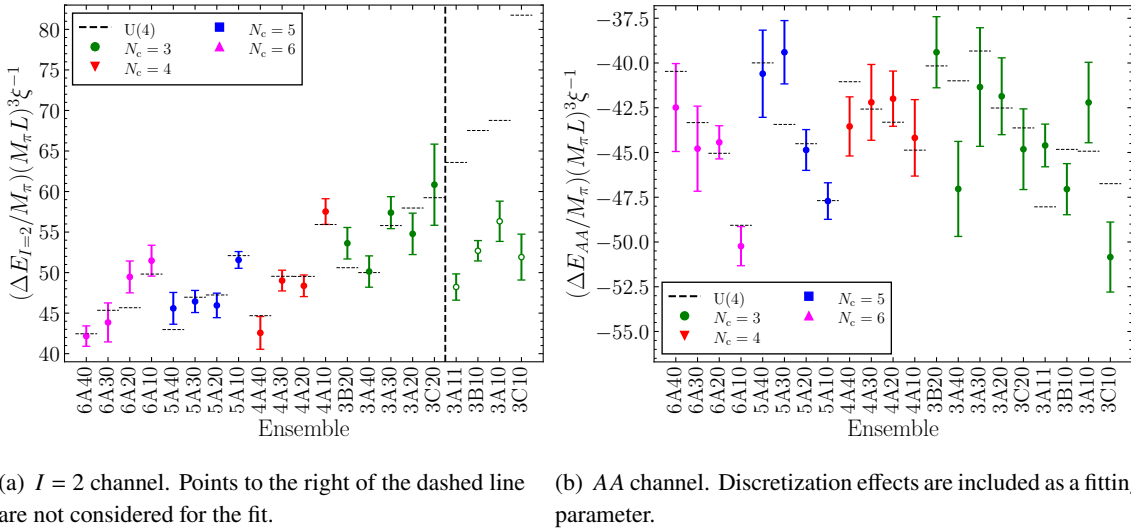


Figure 8: Preliminary results for the simultaneous chiral and N_c fits of the ground state energy shifts to U(4) ChPT.

Because of this, we opt to use the full Lüscher’s formalism and perform a simultaneous chiral and N_c fit to the energy spectrum. The best fits to U(4) ChPT are shown in Fig. 8 for both channels. From these we obtain the following preliminary results for the LECs:

$$\begin{aligned}
L_{I=2}/N_c \times 10^3 &= -0.07(4) - 1.4(2)/N_c, & \chi^2/\text{dof} &= 0.85, \\
L_{AA}/N_c \times 10^3 &= -0.9(2) + 2.6(6)/N_c, & \chi^2/\text{dof} &= 1.34.
\end{aligned}
\tag{15}$$

These values are similar to the ones obtained before from the fits to the scattering length. Still, there is some tension between the leading N_c contribution to the LECs.

6. Summary and outlook

In this talk, we have reported the current status of our study of $\pi\pi$ scattering at Large N_c . We have analyzed the N_c scaling of the scattering amplitudes in the $I = 2$ and AA channels both numerically, and in $U(N_f)$ ChPT up to NNLO. From the comparison of both results, we have extracted the leading and subleading N_c dependence of the relevant LECs.

In future work, we intend to study other scattering channels and meson resonances. The $I = 0$ is very appealing due to the presence of the σ resonance and its contribution to final state interactions in the $K \rightarrow \pi\pi$ decay. However, some preliminary work has shown it is much more computationally expensive. On the other hand, interactions in the AA channel analyzed in this work are attractive, which may lead to the existence of exotic states at higher CM momentum.

7. Acknowledgments

This work has received support from the Generalitat Valenciana grant PROMETEO/2019/083, the European project H2020-MSCA-ITN-2019//860881-HIDDeN, and the national project FPA2017-85985-P. JBB is also supported by the Spanish grant FPU19/04326 of MCIU. FRL acknowledges funding from the European Union Horizon 2020 research and innovation program under the Marie Skłodowska-Curie grant agreement No. 713673 and "La Caixa" Foundation (ID 100010434, LCF/BQ/IN17/11620044). FRL has also received financial support from Generalitat Valenciana through the plan GenT program (CIDEAGENT/2019/040). The work of FRL is supported in part by the U.S. Department of Energy, Office of Science, Office of Nuclear Physics, under grant Contract Numbers DE-SC0011090 and DE-SC0021006. We thank Mare Nostrum 4 (BSC), Finis Terrae II (CESGA), Caléndula (SCAYLE), Tirant 3 (UV) and Lluís Vives (Servei d'Informàtica UV) for the computing time provided.

References

- [1] G. 't Hooft, Nucl. Phys. B **72** (1974) 461.
- [2] P. Hernández and F. Romero-López, Eur. Phys. J. A **57** (2021)2, 52 [hep-lat/2012.03331].
- [3] A. Donini, P. Hernández, C. Pena and F. Romero-López, Eur. Phys. J. C **88**, no. 7, 638 (2020) [hep-lat/2003.10293].
- [4] J. Bijnens and J. Lu, JHEP **2011**, 28 (2011) [hep-ph/1102.0172].
- [5] S. Weinberg, Physica A **96** (1979) 1-2, 327-340.
- [6] J. Gasser and H. Leutwyler, Nucl. Phys. B **250** (1985) 465-516.

- [7] R. Kaiser and H. Leutwyler, Eur. Phys. J. C **17** (2000) 623-649 [hep-ph/0007101].
- [8] M. Lüscher, Commun. Math. Phys. **105** (1986) 153-188.
- [9] M. T. Hansen and S. R. Sharpe, Phys. Rev. D **93** (2016) 014506 [hep-lat/1509.07929].
- [10] L. Del Debbio *et al.*, Phys. Rev. D **80** (2009) 074507 [hep-lat/0907.3896].
- [11] P. Hernández, C. Pena and F. Romero-López, Eur. Phys. J. C **79** (2019) 10, 865 [hep-lat/1907.11511].
- [12] J. Baeza-Ballesteros, P. Hernández and F. Romero-López, in preparation (2021).
- [13] X. Feng, K. Jansen and D. B. Renner, Phys. Lett. B **684** (2010) 268-274 [hep-lat/0909.3255].
- [14] M. I. Buchoff, J.-W. Chen and A. Walker-Loud, Phys. Rev. D **79** (2009) 074503 [hep-lat/0810.2464].
- [15] S. R. Sharpe and J. M. S. Wu, Phys. Rev. D **71** (2005) 074501 [hep-lat/0411021].